Supporting Information

Electron Rearrangement at the Crystalline-Amorphous Heterogeneous Interface Boosts Alkaline Hydrogen Production

Meihuan Liu,[1,+] Yuke Gu,[1,+] Hui Su,[2,*] Xuanzhi Liu,[1] Juan Luo,[1] Pengfei Tan,[1,*] Feng Liu,[3] and Jun Pan[1,3,*]

[1]*State Key Laboratory for Powder Metallurgy, Central South University, Changsha 410083, Hunan, China*

[2]*Key Laboratory of Light Energy Conversion Materials of Hunan Province College, College of Chemistry and Chemical Engineering, Hunan Normal University, Changsha 410081, Hunan, China*
[3]*Yunnan Precious Metals Lab Co., Ltd., Kunming, Yunnan 650106, China*

[+]*These authors contributed equally: Meihuan Liu, Yuke Gu*

* Corresponding authors
E-mail address: suhui@hunnu.edu.cn; tpf0203@csu.edu.cn; jun.pan@csu.edu.cn

Experimental Section

Chemicals. Potassium tetrachloroplatinate (K_2PtCl_4), Cobalt chloride hexahydrate ($CoCl_2·6H_2O$), Nafion solution (5 wt%), and perchloric acid ($HClO_4$, 70%) were purchased from Sigma-Aldrich. KIT-6 molecular sieves were purchased from Jiangsu Xianfeng Nanomaterials Technology Co., Ltd. Sodium hydroxide (NaOH) and L-ascorbic acid (AA) were purchased from Aladdin. All the chemicals were used as received without further purification.

Synthesis of ac-Pt@Co(OH)$_2$: Typically, K_2PtCl_4 (100 mg) and $CoCl_2·6H_2O$ (50 mg) were dispersed in deionized water (10 mL) and ultrasound for 30 min to disperse evenly. 0.5 g KIT-6 was added to the above solution, ultrasound for another 1 hour and further dried under vacuum to obtain a powder (percursor@KIT-6). After that, 2 mL of 1 M AA solution was added dropwise to the powder and undisturbed for 48 h. Finally, the percursor@KIT-6 was added into 2M hot NaOH for continuous stirring to remove the KIT template. Black powder was centrifuged and washed with distilled water.

Synthesis of c-Pt: The synthesis route was similar to that of ac-Pt@$Co(OH)_2$, except without adding $CoCl_2·6H_2O$.

Material characterization

Transmission electron microscopy (TEM), high-resolution transmission electron microscopy (HRTEM), and energy dispersive X-ray spectroscopy (EDX) were performed on a Talos F200X instrument. The powder X-ray diffraction (XRD) patterns were measured in a Philips X'Pert Pro Super X-ray diffractometer with Cu K_α radiation (λ = 1.54178 Å). ThermoFisher-VG Scientific (ESCALAB250X) was applied to gather the X-ray photoelectron spectroscopy (XPS), and all the binding energies obtained in XPS spectra analysis were corrected by C 1*s* at 284.8 eV. The Pt *L*-edge and Co *K*-edge X-ray absorption spectra were measured at the BL20 U station in the Shanghai Synchrotron Radiation Facility (SSRF, China).

Electrochemical measurements

Electrochemical measurements of HER performance were performed in a standard three-electrode system from Pine Research Instrumentation. The working electrode was a glassy carbon rotating disk electrode (RDE) coated with catalysts. The saturated Hg/HgO (1 M KOH) and carbon rod were employed as the reference and counter electrodes, respectively. The electrocatalysts were dispersed in a mixture solution (730 μL deionized water, 250 μL ethanol, and 20 μL Nafion) and then sonicated to form homogeneous inks. Before the linear sweep voltammetry (LSV) test in 1 M KOH electrolyte, all electrodes were activated by the cyclic voltammetry (CV) techniques for 100 cycles to obtain stable LSV curves. The as-prepared ink was dropped onto the glassy carbon (GC) disk of the RDE to receive a loading of 25 μg_{Pt} cm^{-2} for all the catalysts. LSV curves were conducted in 1.0 M KOH electrolyte at a scan rate of 5 mV/s with 95% iR-compensation under a rotation speed of 1600 rpm. Accelerated durability tests (ADT) were performed on RDE by measuring CV curves between 0.1 to -0.5 V vs RHE for 20000 circles at a sweep rate of 100 mV s^{-1}. The long-term stability tests of the catalysts were also assessed by CP under 100 mA cm^{-2} for 100 h via coating the catalysts on carbon paper with a loading of 50 μg_{Pt} cm^{-2}. Electrochemical impedance spectroscopy (EIS) measurements were determined at an overpotential of 50 mV in the frequency range of 0.1–100 000 Hz.

In situ XAFS measurements

In situ XAFS measurements were performed with catalyst-coated carbon cloths in an alkaline solution using a smart homemade cell through a three-electrode system. In particular, 10 mg sample was uniformly dispersed in a 1 mL solution (0.5 mL ethanol and 0.5 mL deionized water) with 20 μL Nafion. Then, the catalyst ink was dropped onto the carbon paper as the working electrode (~1cm × 1cm), and the back of the carbon paper was fixed with Capton film to ensure that all electrocatalysts could react with the electrolyte. A series of representative voltages were applied to the electrode to capture the dynamic evolution information of the active site during the electrochemical reaction. For the *in situ* XAFS spectra acquisition of Pt *L*-edge and Co *K*-edge, we calibrated the positions of absorption edges (E_0) by using Pt foil and Co foil standard samples, respectively, and all XAFS data were collected during one period of beam time. The acquired EXAFS data were processed according to the standard procedures using the ATHENA module implemented in the IFEFFIT software packages. Subsequently, k^2-weighted and k^3-weighted $\chi(k)$ data in the k-space ranging from 2.7–11.7 $Å^{-1}$ and 2.5–11.2 $Å^{-1}$ were Fourier transformed to real space using a Hanning window (dk = 1.0 $Å^{-1}$) to separate the EXAFS contributions from different coordination shells for Pt and Co samples, respectively.

Density functional theory (DFT) calculation

All DFT calculations were performed using the Vienna Ab-initio Simulation Package (VASP). The Perdew-Burke-Ernzerhof (PBE) function of the Generalized Gradient Approximation (GGA) was used to describe the exchange-correlation energy, and the ion-electron interactions were represented by the projector-augmented wave (PAW) method. The Kohn-Sham valence states were expanded in a plane-wave basis set with a cut-off energy of kinetic energy cutoff of 450 eV. The geometry optimization was performed when the convergence criterion on forces became less than 0.02 eV/Å with the electronic relaxation threshold of 10^{-5} eV. The calculated Fermi energy was set to zero for all the DOS plots. In addition, the calculation of amorphous/crystalline boundary was conducted using ab initio molecular dynamics (AIMD).

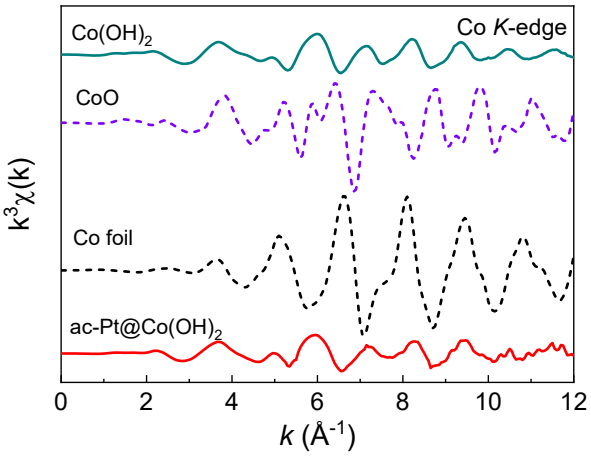

Figure S1. The $k^3\chi$ (k) oscillation curve of Co K-edge in ac-Pt@$Co(OH)_2$.

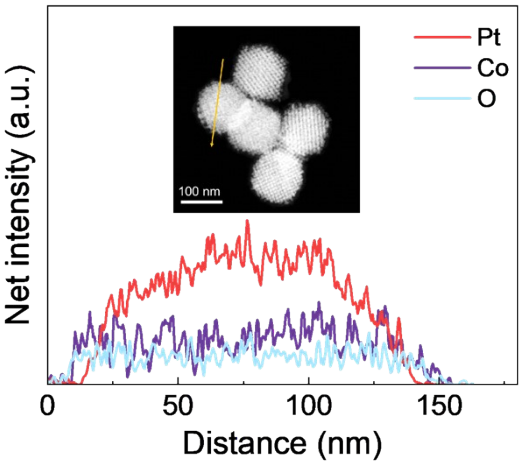

Figure S2. Line scanning curves of ac-Pt@$Co(OH)_2$, inset is the HADDF-TEM image.

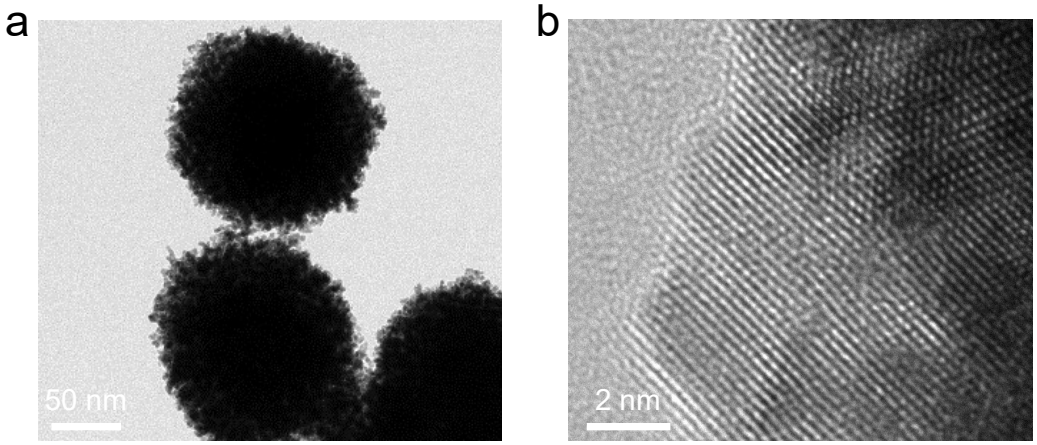

Figure S3. (a) TEM and (b) HRTEM images of c-Pt.

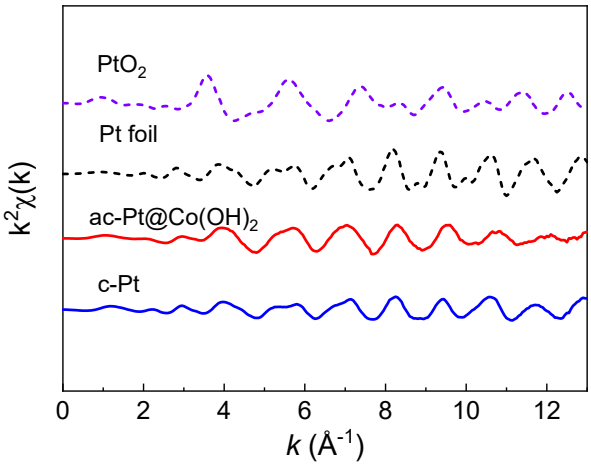

Figure S4. The $k^2\chi$ (k) oscillation curve of Pt L-edge in ac-Pt@$Co(OH)_2$.

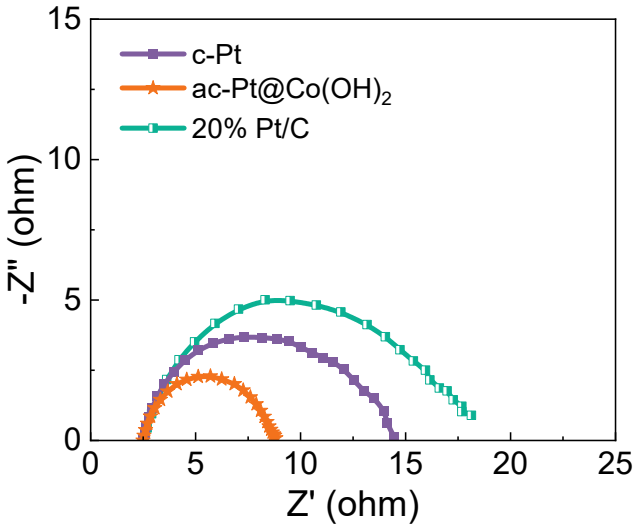

Figure S5. Nyquist plots of electrochemical impedance spectra of c-Pt, ac-Pt@$Co(OH)_2$, and Pt/C catalysts.

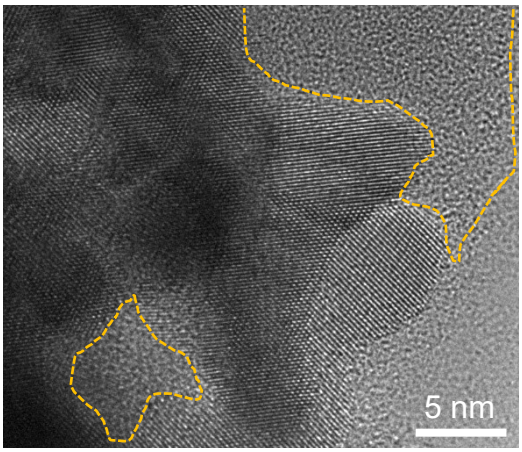

Figure S6. HRTEM images for ac-Pt@$Co(OH)_2$ after stability testing.

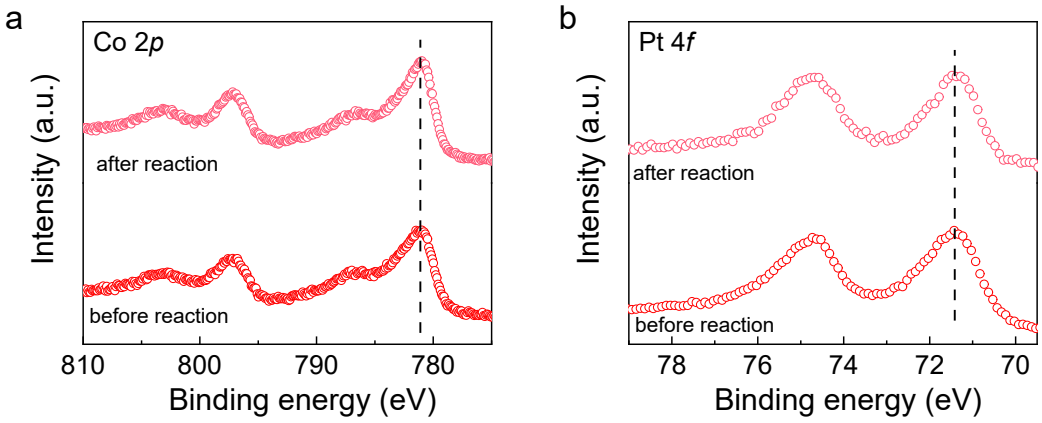

Figure S7. (a) Co 2*p* and (b) Pt 4*f* XPS spectra before and after stability testing for ac-Pt@Co(OH)$_2$.

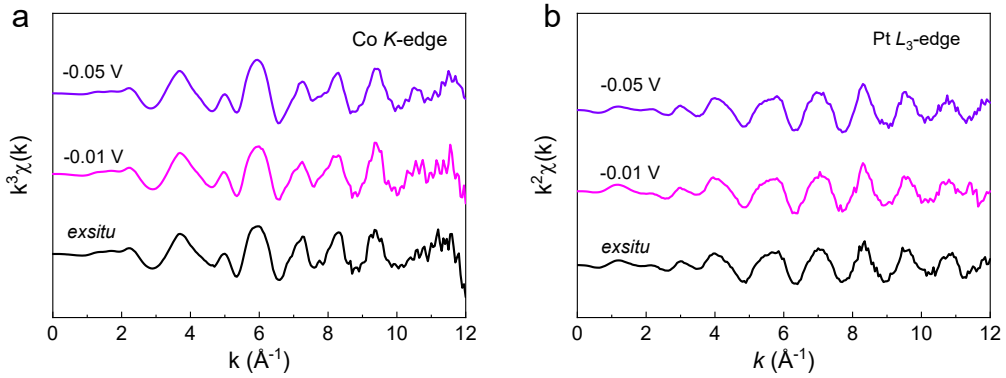

Figure S8. (a) $k^3\chi$ (k) oscillation curve of Co K-edge and (b) $k^2\chi$ (k) oscillation curve of Pt L-edge for ac-Pt@Co(OH)$_2$ under *in situ* conditions.

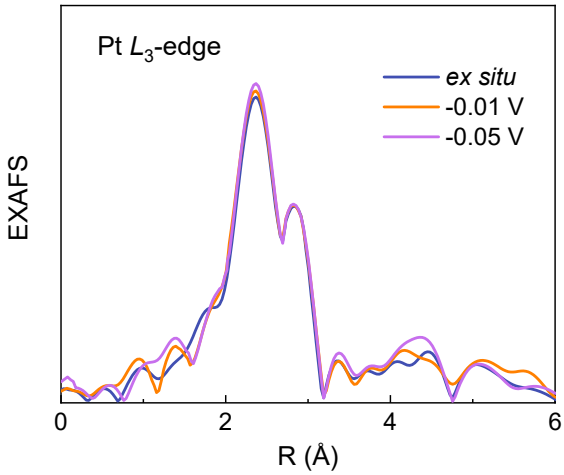

Figure S9. *In situ* EXAFS spectra of Pt L_3-edge in ac-Pt@Co(OH)$_2$.

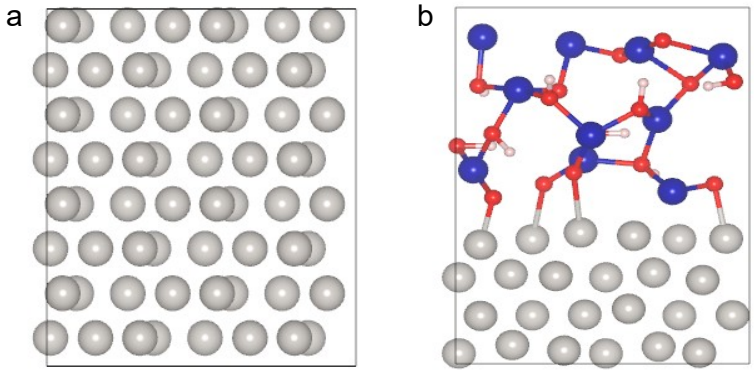

Figure S10. The structure model of (a) c-Pt, and (b) ac-Pt@$Co(OH)_2$. Gray, blue, red, and light pink balls represent Pt, Co, O, and H atoms.

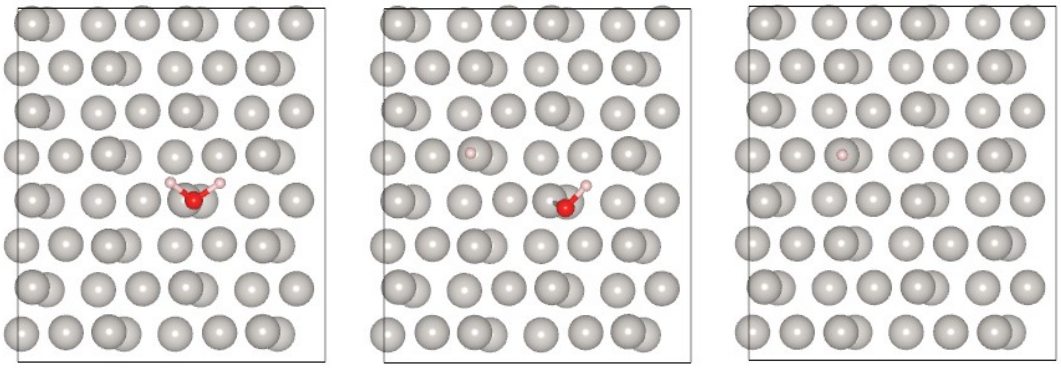

Figure S11. Configurations of adsorbed intermediates (*H_2O, *OH, *H) on c-Pt.

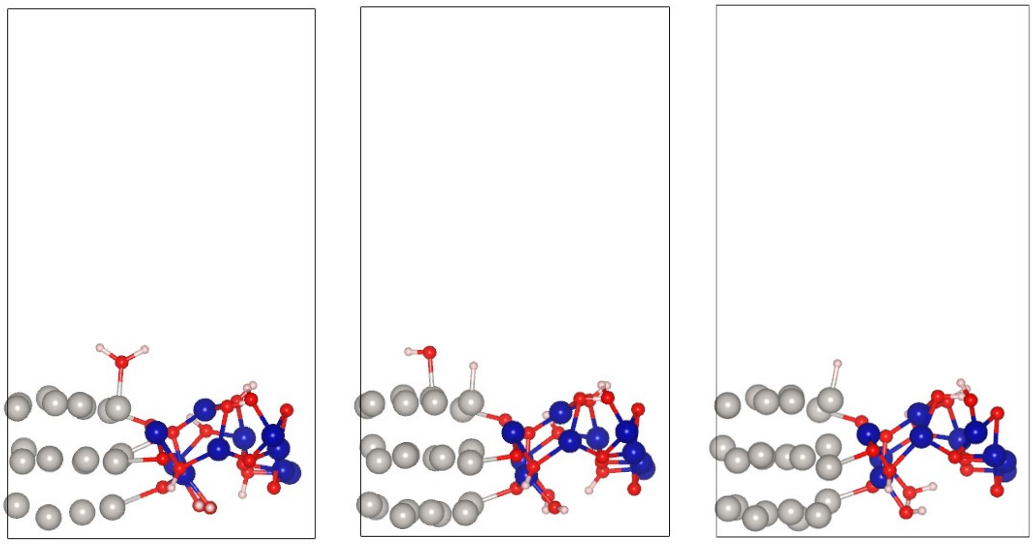

Figure S12. Configurations of adsorbed intermediates (*H_2O, *OH, *H) on **a**c-Pt@$Co(OH)_2$, where *H_2O was absorbed over Pt site.

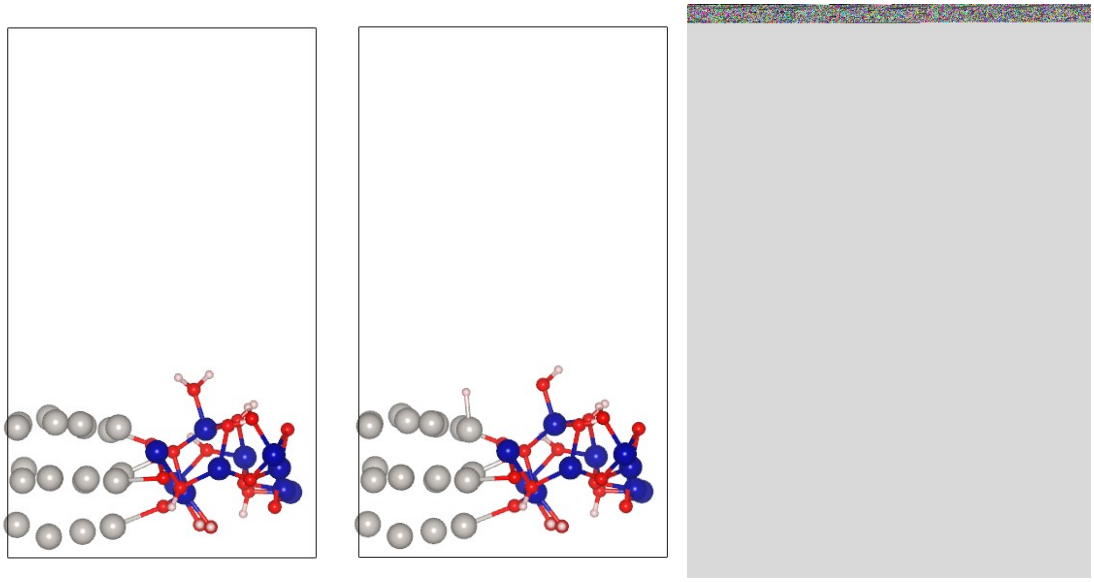

Figure S13. Configurations of adsorbed intermediates (*H_2O, *OH, *H) on **a**c-Pt@$Co(OH)_2$, where *H_2O was absorbed over Co site.